

ADVANCES IN FOREST FIRE RESEARCH

2022

Edited by

**DOMINGOS XAVIER VIEGAS
LUÍS MÁRIO RIBEIRO**

Effect of Fuel Bed Structure on the Controlling Heat Transfer Mechanisms in Quiescent Porous Flame Spread

Zakary Campbell-Lochrie*¹; Carlos Walker-Ravena¹; Michael Gallagher²; Nicholas Skowronski³;
Eric V. Mueller¹; Rory M. Hadden¹

¹The University of Edinburgh, Edinburgh, UK,

{z.campbell.lochrie, c.walkerravena, R.Hadden}@ed.ac.uk, {ericvmueller@gmail.com}

²Northern Research Station, USDA Forest Service, New Lisbon, NJ, USA {Michael.r.gallagher@usda.gov}

³Northern Research Station, USDA Forest Service, Morgantown, WV, USA

{Nicholas.s.skowronski@usda.gov}

*Corresponding author

Keywords

Flame spread, fuel structure, heat transfer, fire modelling, thermal model

Abstract

The increasing importance of prescribed fire use has led to an increased focus on the development of modelling tools suited to conditions typical of prescribed fire scenarios. An improved understanding of flame spread through porous surface fuels represents an important part of these efforts. In the lower wind speed conditions typical of many prescribed burns, the role of fuel structure may be of greater importance than in highly wind-aided flame spread scenarios. The porous nature of wildland fuel beds complicates efforts to apply existing, solid surface theories for flame spread in low or quiescent wind conditions as radiation, convection and conduction may all occur within the porous fuel in addition to flame heating. An important first step in the development of any flame spread theory is the identification of the dominant heat transfer mechanisms but for wildland fuels the effect of fuel structure on the relative importance of different heating mechanisms must be considered. To investigate the role of fuel structure we therefore present a series of laboratory-based flame spread experiments conducted in pine needle fuel beds with various structural properties. The fuel loading and bulk density were independently varied by controlling fuel bed height with water-cooled heat flux gauges used to measure the (radiant and total) heat flux from both the above-bed flame and the in-bed combustion region. A single dimensionless parameter ($\alpha\sigma\delta$), incorporating the fuel bed porosity (α), fuel element surface-to-volume ratio (σ), and fuel bed height (δ), was used to describe the overall fuel bed structure. The heat flux measurements highlighted the dominant role of in-bed heating across all of the studied fuel conditions although the magnitude of above-bed flame heating increased with increasing fuel loading. Heat fluxes from the in-bed combustion region exceeded those from the above-bed flame region with the magnitude of the peak (radiant and total) heat flux at each measurement location generally increasing with increasing $\alpha\sigma\delta$ across the studied range ($\alpha\sigma\delta = 49$ to 399). However, the effect of fuel loading was also apparent with a positive relationship also observed between fuel loading and flame height. The experimentally observed effective heating distances also varied with bulk density and fuel loading and were used to evaluate the use of a thermal modelling approach incorporating the bulk structural properties of the porous fuel bed. Comparison with experimental observations of spread rate indicated a maximum variation in predicted spread rate of 29 % where only radiative transfer from the in-bed combustion region was considered, with closer agreement at lower $\alpha\sigma\delta$ values. Where the contributions of both the in-bed and above-bed heat transfer mechanisms were considered, the need to incorporate additional heat loss terms into this thermal model were apparent. This study therefore emphasises the important role of porous fuel structure on the in-bed heat transfer and assesses suitable, physically meaningful structural descriptors. The experiments presented in this study will also provide a valuable dataset for future model development efforts incorporating measurements of fire behaviour and underlying physical phenomena across a wide range of structural conditions.

1. Introduction

Flame spread dynamics in quiescent/low-wind conditions typical of many prescribed fire scenarios differ compared to wind-driven wildfires particularly as the dominant heat transfer modes may change, altering the pre-heating of fuels ahead of the flame front. Differences in fire behaviour challenge existing model tools (Hiers *et al.*, 2020) and have motivated recent physics-based model development efforts (Gallagher *et al.*, 2021). However, semi-empirical models (e.g. Rothermel's model) underpin many simulation models (Andrews, 2018).

Rothermel's model (Rothermel, 1972) involves application of the energy conservation principle to a unit volume of fuel ahead of the flame front. This results in an expression for the rate of spread equal to the ratio between the propagating heat flux and the net heat required for ignition of the fuel. In the development of the Rothermel model, an analytical solution of this energy balance could not be made as the heat transfer mechanisms associated with these heat flux terms was unknown therefore the development of empirical terms was required for model closure.

Identification of the dominant heat transfer mechanism(s) is an important first step in the development of any flame spread theory (Williams, 1977). The porous structure of wildland fuels allows radiative and convective heat transfer to occur within the fuel bed. Appropriate descriptors of porous fuel bed structure which can be related to variations in both above-bed and in-bed heat transfer processes are therefore required. Several studies have measured heat fluxes in/near wildland fuels however analysis of the relative importance of heat transfer mechanisms and the effect of fuel structure is restricted by the wide variety of measurement types and locations limiting inter-study comparisons (Frankman *et al.*, 2010).

In the present study, heat transfer in pine needle fuel beds (heat fluxes from both from the trailing combustion region and the overhead flame) were investigated experimentally. Fuel loading and bulk density were independently varied by controlling the fuel bed height with fuel bed structure also described by the dimensionless parameter $\alpha\sigma\delta$ which incorporates porosity (α), surface-to-volume ratio (σ), and fuel height (δ) (Campbell-Lochrie *et al.*, 2021). A simple thermal modelling approach, incorporating the experimentally measured heat fluxes and heating distances, is used to explore the relative importance of different heating sources.

2. Methods

Experiments involved a flame spread table (1.5 m by 0.67 m) with vermiculite substrate and insulated sidewalls (extending 0.03 m above fuel height). Gas phase temperature measurements (0.25 mm dia. K-Type thermocouples) and video analysis enabled characterisation of fire behaviour (spread rate, flame height). Heat Release Rate (HRR) was calculated using oxygen consumption calorimetry. 10 ml of acetone, distributed equally over a 0.67 m length of alumina-silica fibre, provided a line ignition source.

Heat fluxes from the flame and the in-bed combustion region were measured using water-cooled heat flux gauges (calibrated up to 100 kW/m²). Windowed (sapphire lens with spectral transmission range of 0.2 – 5.5 μ m) and exposed gauges were co-located to measure radiant and total heat flux respectively. Two different experimental setups were employed (as shown in Figure 1) allowing measurement of both horizontal heat flux through the fuel bed and vertical heat fluxes to/through the fuel bed.

The first series involved four heat flux gauges (two pairs of co-located windowed and exposed gauges) positioned vertically (sensor face parallel to fuel bed surfaces) at a horizontal distance of 1.3 m from the ignition line (0.2 m from the end of the fuel bed). One pair was positioned flush to the table surface (exposed to above-bed flame heating) while the second pair was positioned flush with the fuel bed surface (exposed to both above-bed and in-bed heating). In-bed thermocouples were positioned at a distance of 0.3 m, 0.6 m and 0.9 m from the ignition line.

In the second series, two heat flux gauges (windowed and exposed pair) were used. Gauges were positioned to measure the horizontal heat flux (sensor face perpendicular to fuel bed surfaces) and located within the fuel bed (midpoint of the gauge at a height of 12.7 mm above the table surface). Gauges primarily measured heat fluxes from the in-bed combustion region transferred horizontally through the fuel bed. Gauges were located at a horizontal distance of 0.9 m from the ignition line (0.6 m from the end of the fuel bed). Above-bed thermocouples were positioned at distances of 0.6 m, 0.8 m, 0.85 m and 0.9 m from the ignition line.

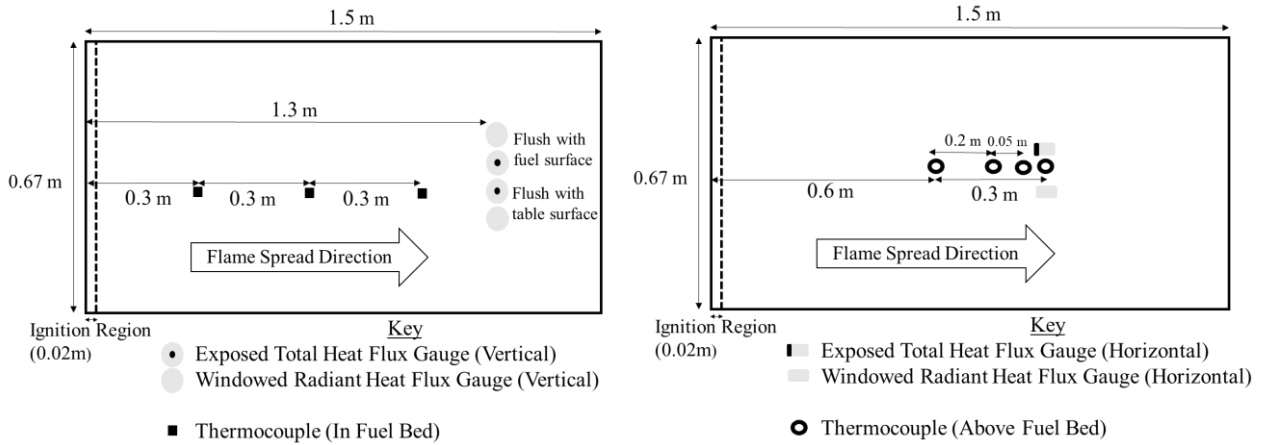


Figure 1. (left) 1st experimental setup involving four vertical heat flux gauges [sensor faces parallel to fuel bed surfaces] (right) 2nd experimental setup involving two horizontally-oriented heat flux gauges [sensor faces perpendicular to fuel bed surfaces]

Fuel beds (1.5 m by 0.67 m) were composed of pitch pine (*Pinus rigida* Mill.) needles (density = $706 \pm 71 \text{ kg/m}^3$, surface-to-volume ratio = $5063 \pm 640 \text{ m}^{-1}$) collected in the New Jersey Pinelands National Reserve. The dead needles had an average Fuel Moisture Content (FMC) of $13.2 \% \pm 4.6 \%$. Fuel bed structure was varied by altering fuel loading (0.2 to 1.6 kg/m^2), bulk density (10 to 40 kg/m^3), and fuel height (10 to 80 mm).

3. Results & Discussion

3.1. Overall Observations

A positive correlation between spread rate and fuel loading, and a negative correlation between spread rate and bulk density were observed, as shown in Table 1. Positive relationships between spread rate and $\alpha\sigma\delta$ ($R^2 = 0.91$) and between flame height and spread rate ($R^2 = 0.86$) were also observed.

Table 1. Summary of fire behaviour observations

Fuel Loading [kg/m^2]	Bulk Density [kg/m^3]	α	δ [mm]	$\alpha\sigma\delta$	N	Flame Spread Rate [mm/min \pm Max/Min]	Flame Height [m \pm 0.05 m]	Peak HRR [kW \pm Max/Min]
0.2	20	0.972	10	49	2	82 ± 17	0.05	4.5 ± 2.4
0.4	10	0.986	40	200	2	168 ± 16	0.23	24.5 ± 5.0
0.4	20	0.972	20	98	4	114 ± 24	0.13	15.6 ± 1.7
0.6	20	0.972	30	148	2	139 ± 20	0.29	19.5 ± 5.0
0.8	10	0.986	80	399	4	195 ± 37	0.55	38.3 ± 1.0
0.8	20	0.972	40	197	5	149 ± 30	0.36	31.7 ± 1.8
0.8	40	0.943	20	96	4	122 ± 47	0.34	20.7 ± 1.0
1.2	20	0.972	60	295	2	198 ± 18	0.55	69.2 ± 6.9
1.6	20	0.972	80	394	4	206 ± 67	0.74	120.3 ± 12.3

3.2. Heat Fluxes

As shown in Figure 2, except where negligible heat flux was measured, heat flux profiles typically consisted of an initial steady growth period followed by a sharp rate of increase prior to a period of peak-decay behaviour.

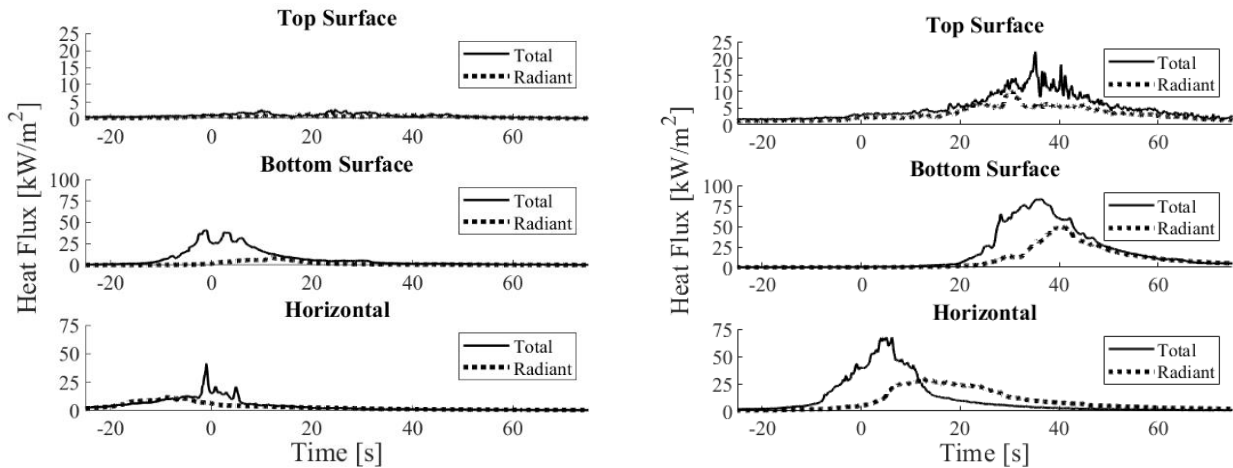


Figure 2. Characteristic total heat flux profiles at each gauge location for fuel beds of (left) $\alpha\sigma\delta = 98$ and (right) $\alpha\sigma\delta = 197$

Across all fuel conditions, heat transfer from the in-bed combustion region was the dominant heat transfer path in this flame spread scenario (compare top surface with bottom surface and horizontal measurements in Figure 2). In the first experimental series, the ratio of peak total heat flux measured at the bottom surface to that measured at the top fuel bed surface, ranged from 2.2 to 14 across the studied conditions. In-bed heating as measured by the horizontal gauges (heat transferred horizontally through the fuel bed from the combustion region) exceeded flame heating from the above-bed flame (measured at the top surface of the fuel bed), as shown in Figure 3.

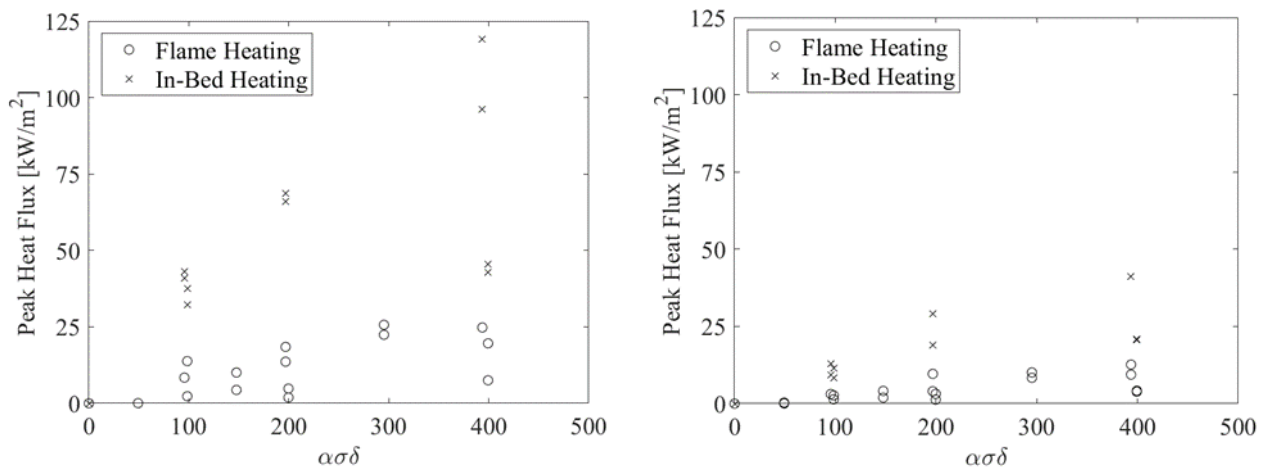


Figure 3. Comparison of peak (left) total and (right) radiant heat flux from the above-bed flame (flame heating) with horizontal heat flux through fuel beds (in-bed heating) of various structures

As shown in Figure 3, heat fluxes varied between fuel beds of different fuel structure ($\alpha\sigma\delta$). Generally, higher peak fluxes (radiant and total) occurred in fuel beds of higher $\alpha\sigma\delta$ values. However, the importance of fuel loading at similar $\alpha\sigma\delta$ values is observed in the two highest $\alpha\sigma\delta$ cases ($\alpha\sigma\delta=394$ and $\alpha\sigma\delta=399$), with significant variation in heat flux magnitudes occurring between these cases. The heat flux from the overhead flame increased with fuel loading which is in line with the positive relationship observed between fuel loading and flame height. Effective heating distance through the fuel bed is dependent upon porosity and attenuation characteristics of the fuel bed and varied with fuel loading and bulk density.

3.3. Thermal Model

A thermal model was constructed based on assumed bulk fuel bed properties, following an energy conservation approach similar to those previously described for porous fuel beds (Frandsen, 1971) and thermally thin solids (Quintiere, 2006). A control volume was defined within the fuel bed and fixed to the pyrolysis front position (x_p) as shown in Figure 4 with the flame spread rate described by:

$$v_p = \frac{\int_{x_p}^{\infty} \dot{q}_p''(x) dx + \int_{x_p}^{\infty} \dot{q}_f''(x) dx}{\rho c_p \delta (T_{ig} - T_s)}$$

where \dot{q}_p'' is the heat flux into the control volume from the combustion region (integrated across the effective heating length), \dot{q}_f'' is the heat flux from the above-bed flame, T_{ig} and T_s are the ignition and initial fuel temperatures respectively, and δ is the fuel height. Bulk fuel bed properties were based upon volume-averaged air and needle properties (density (ρ) and specific heat capacity (c_p)). Both \dot{q}_p'' and \dot{q}_f'' were integrated across their respective effective heating distances which were determined experimentally based upon the time between onset of heating at the heat flux gauge (0.5 kW/m² threshold) and the time of peak heat flux. Similarly, heat flux magnitude is based on experimental values, with 1 s moving average applied.

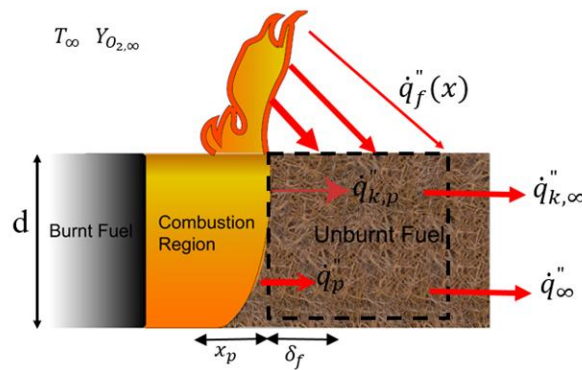


Figure 4. Schematic of control volume for flame spread model

Considering only radiative heat flux from the combustion region results in similar predicted Rate of Spread (ROS) values to those observed experimentally. A maximum variation between the predicted ROS and the experimentally measured ROS of 29 % was observed, with closer agreement for fuel beds of lower $\alpha\sigma\delta$ values, as shown in Figure 5. Given the greater HRR values in fuel beds of higher $\alpha\sigma\delta$ values, it may be that greater entrainment increases the convective cooling, with these heat losses not accounted for in this model.

Considering instead heat transfer only from the flame results in an underestimation of the ROS, particularly in fuel beds of lower $\alpha\sigma\delta$ values. This suggests that the dominance of the heat transfer from the combustion region increases at lower $\alpha\sigma\delta$ values. The predicted ROS is also shown where both the combustion region and flame heat transfer are included in the thermal model. This tends to overestimate the ROS, compared to experimental observations, however the effect of convective cooling (or radiative losses) is not considered and therefore this over-estimate is not unexpected and is in line with previous studies (De Mestre *et al.*, 1989).

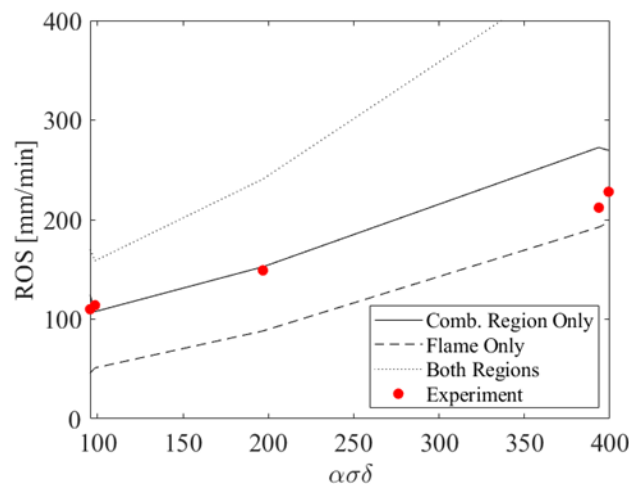


Figure 5. Comparison of avg. experimental Rate of Spread (ROS) values and thermal model ROS predictions for cases considering radiant heat flux from combustion Region only, flame region only, and both regions

4. Conclusions

By varying the structure of porous fuel beds (fuel loading, bulk density, fuel bed height), fuel loading and bulk density were observed to independently influence flame spread rate and fire behaviour (flame height, heat release rate). The effect of fuel structure on flame spread rate was well-described by the parameter $\alpha\delta$. Examining further the underlying physical mechanisms controlling the flame spread process highlighted the dominant role of in-bed heat transfer (from the combustion region in the fuel bed) across the range of fuel beds studied ($\alpha\delta = 49$ to $\alpha\delta = 399$). The significance of heat transfer contributions from the overhead flame generally increased with increasing $\alpha\delta$ value of the fuel bed, in contrast with some past predictions regarding heat transfer mechanisms in shallow fuel beds. Direct measurement of heat flux and effective heating distance, allowed development of a simple thermal model considering only radiative heating contributions. Comparison with experimental observations of spread rate indicated a maximum variation in predicted ROS of 29 % where only radiative transfer from the in-bed combustion region was considered, with closer agreement at lower $\alpha\delta$ values. Where the contributions of both the in-bed and above-bed heat transfer mechanisms were considered, the need to incorporate appropriate heat loss terms into this thermal model was apparent.

5. References

- Andrews, P.L. (2018) The rothermel surface fire spread model and associated developments: A comprehensive explanation. U.S. Forest Service. Rocky Mountain Research Station. General Technical Report RMRS-GTR-371.
- Campbell-Lochrie, Z., Walker-Ravena, C., Gallagher, M., Skowronski, N., Mueller, E.V., Hadden, R.M. Investigation of the role of bulk properties and in-bed structure in the flow regime of buoyancy-dominated flame spread in porous fuel beds, *Fire Saf. J.* (2021). doi:10.1016/j.firesaf.2020.103035.
- De Mestre, N.J., Catchpole, E.A., Anderson, D.H., Rothermel, R.C. Uniform Propagation of a Planar Fire front Without Wind, *Combust. Sci. Technol.* 65 (1989) 231–244. doi:10.1080/00102208908924051.
- Frandsen, W. H. (1971). Fire spread through porous fuels from the conservation of energy. *Combustion and Flame*, 16(1), 9-16.
- Frankman, D., Webb, B.W., Butler, B.W., Time-resolved radiation and convection heat transfer in combusting discontinuous fuel beds, *Combust. Sci. Technol.* 182 (2010) 1391–1412. doi:10.1080/00102202.2010.486388.
- Gallagher, MR., Cope, Z., Giron, D.R., Skowronski, N.S., Raynor, T., Gerber, T., Linn, R.R., Hiers, J.K., Reconstruction of the Spring Hill Wildfire and Exploration of Alternate Management Scenarios Using QUIC-Fire. *Fire*. 2021; 4(4):72. <https://doi.org/10.3390/fire4040072>
- Hiers, J.K., O'Brien, J.J., Varner, J.M., Butler, B.W., Dickinson, M., Furman, J., Gallagher, M., Godwin, D., Goodrick, S.L., Hood, S.M. Prescribed fire science: the case for a refined research agenda. *Fire Ecology*, 16(1), 1-15 (2020). <https://doi.org/10.1186/s42408-020-0070-8>
- Rothermel, R. C. (1972). A mathematical model for predicting fire spread in wildland fuels (Vol. 115). Intermountain Forest & Range Experiment Station, Forest Service, US Department of Agriculture.
- Quintiere, J.G. *Fundamentals of Fire Phenomena*, 2006. doi:10.1002/0470091150
- Williams, F.A. Mechanisms of fire spread, *Symp. Combust.* 16 (1977) 1281–1294. doi:10.1016/S0082-0784(77)80415-3.